

A SAMPLE PARTITIONING APPROACH FOR MILLING STABILITY MODELING WITH CHATTER FREQUENCY TEST POINT SELECTION

Tony Schmitz
Machine Tool Research Center
University of Tennessee, Knoxville
Knoxville, TN, USA

INTRODUCTION

For discrete part production by milling, the optimum combination of spindle speed and axial depth is desired to maximize material removal rate (MRR) and minimize cost. To identify the optimal {spindle speed, axial depth} combination that provides maximum MRR without chatter, a self-excited vibration, analytical and numerical milling models are available [1]. These models have two primary inputs: 1) the tool tip frequency response function, FRF; and 2) a cutting force model that relates the cutting force to the commanded chip area using mechanistic coefficients. The tool tip FRF may be measured using tap testing, where an instrumented hammer is used to excite the tool tip and a linear transducer, such as a low-mass accelerometer, is used to measure the response. The measured tool tip FRF can then be represented by a discrete number of vibration modes, each of which is described by a natural frequency, modal stiffness, and modal damping ratio. The cutting force model coefficients may be identified experimentally by measuring the cutting force for known milling parameters and determining the least squares best fit coefficients using the force model and measured force.

The objective of this research is to increase milling stability model accuracy when the inputs are initially uncertain. Uncertainties in two inputs are considered: the modal parameters that represent the tool tip FRFs and the cutting force model coefficients.

SAMPLE PARTITIONING

A sample partitioning approach is proposed to reduce uncertainty in: 1) modal parameters that represent the tool tip FRF; and 2) cutting force model coefficients using milling stability tests. The approach is to partition stability maps that agree with sequential stability tests completed at selected {spindle speed, axial depth} combinations from those that disagree. The stability maps are generated using the zero-order frequency domain stability model [2]. Tests are

performed using time domain simulation, where the time-delay differential equations of motion that represent the milling system are solved numerically. Because the zero-order frequency domain stability model inputs (i.e., the modal parameters and cutting force coefficients) are uncertain, Monte Carlo simulation is applied to randomly sample distributions of the inputs to predict many potential stability maps. Each stability map represents one sample that may or not be the true map; all samples have an equal probability of being the true stability map.

The selection of test points is based on the outcome of the previous test (i.e., stable or unstable/chatter behavior is exhibited). If the previous test was stable, the next test is selected where maximum expected MRR is obtained. To determine the test point in this case, the mean axial depth from all available stability maps (after partitioning based on the previous stable result) is identified for each spindle speed. The MRR is then calculated using the mean axial depth at the selected spindle speed. After repeating the calculation for each spindle speed, the {spindle speed, axial depth} combination that gives the maximum MRR is chosen as the next test point.

If the previous test was unstable, the chatter frequency is determined by converting a time domain milling signal, such as force or displacement, to the frequency domain. In the frequency domain, chatter is identified when content appears at frequencies other than the tooth passing frequency, f_{tooth} , and its multiples (harmonics); see Eq. 1, where Ω is the spindle speed (rpm) and N_t is the number of teeth on the endmill. The chatter frequency, f_c (Hz), is applied to calculate the next spindle speed, Ω (rpm), using Eq. 2. By comparing Eqs. 1 and 2, it is observed that the spindle speed for the next test is selected by setting the new tooth passing frequency equal to the chatter frequency from the previous test [3].

$$f_{tooth} = \frac{\Omega N_t}{60} \quad (1)$$

$$\Omega = \frac{60f_c}{N_t} \quad (2)$$

After partitioning the maps based on stability tests, those maps that agree with the tests are used to identify the most likely input values and reduce the associated uncertainty since there is a one-to-one correspondence between the maps and the modal parameters and cutting force model coefficients; see Fig. 1.

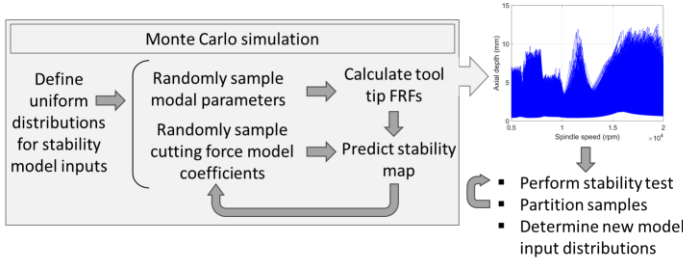


FIGURE 1. Sample partitioning using stability testing.

The sample partitioning algorithm is described by Fig. 2, which displays many potential stability boundaries (i.e., the family of blue curves) generated by Monte Carlo simulation. Consider the test at the {spindle speed, axial depth} pair labeled $\{\Omega_u, b_u\}$. As indicated by the u subscript and the red x , the test result is unstable. The stability boundaries are partitioned using this test result. Those that predict an unstable result (agree) are separated from those that predict a stable result (disagree). Only those sample boundaries that agree are retained. This means that all boundaries with a limiting axial depth greater than b_u are eliminated.

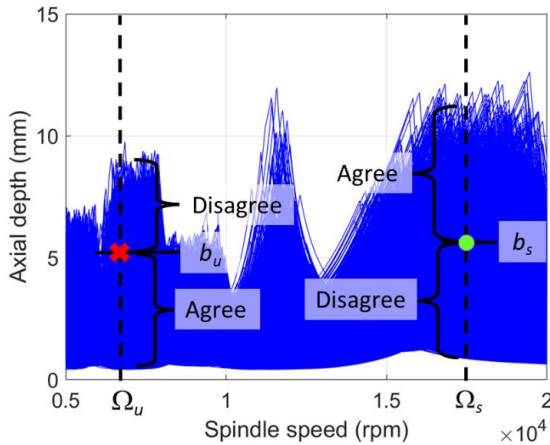


FIGURE 2. Sample partitioning algorithm description.

Next, consider the test at $\{\Omega_s, b_s\}$. As indicated by the s subscript and the green circle, the test result is stable. In this case, all boundaries with a limiting axial depth greater than b_s at Ω_s are retained (agree) and boundaries with a limiting axial depth less than b_s at Ω_s are eliminated (disagree) from the distribution. The sample partitioning is repeated sequentially for all tests, both stable and unstable, to refine the initial distributions of not only the stability maps, but also the modal parameters and cutting force model coefficients. Specifically, each map that disagrees with the test result and is eliminated also eliminates the corresponding values of the modal parameters and cutting force model coefficients used to produce that map. This enables the initial distributions of these uncertain parameters to be refined and, subsequently, the uncertainty in the parameters and stability predictions to be reduced.

TABLE 1. True values for stability model inputs.

Modal parameters			
f_{n1} (Hz)	1000	f_{n2} (Hz)	1200
k_1 (N/m)	5×10^6	k_2 (N/m)	7×10^6
ζ_1 (-)	0.02	ζ_2 (-)	0.03
Cutting force model coefficients			
k_t (N/mm ²)	700		
k_n (N/mm ²)	200		

CASE STUDY

To evaluate the proposed sample partitioning algorithm and test selection approach, a numerical study was completed where the stability maps were predicted using the frequency domain stability model [1] and test data was collected using the results of milling time domain simulation [3]. For the milling stability tests, a 12.7 mm diameter, four-tooth endmill with a 30 deg helix angle and uniform teeth spacing was selected. The radial depth was 3 mm and the feed per tooth was 0.1 mm for the down milling, x direction milling tests; the spindle speed and axial depth were varied to partition the predicted stability maps using the test results (labeled stable or unstable). The true modal parameters are provided in Table 1; two modes were selected and the FRFs were symmetric in the x and y directions. The true cutting force coefficients are also listed in Table 1; these are representative of a 6061-T6 aluminum workpiece material.

Stability was determined using the x direction displacement predicted by the time domain simulation. The time dependent displacement

was converted to the frequency domain and the chatter frequency was identified, if present. As noted, the frequency content from each test was compared to the tooth passing frequency (i.e., the spindle speed multiplied by the number of flutes) and its integer multiples (harmonics). A test was labeled as stable if content appeared only at these frequencies. A test was labeled as unstable if frequency content was observed at a different frequency and the chatter frequency was recorded for selection of the next test point.

For the two-mode system, chatter can occur either in the 1000 Hz mode or the 1200 Hz depending on which portion of the stability boundary is exceeded. This is demonstrated in Fig. 3, where it is observed that exceeding the stability boundary to the right of the peak at 15620 rpm results in a different chatter frequency than exceeding the boundary to the left.

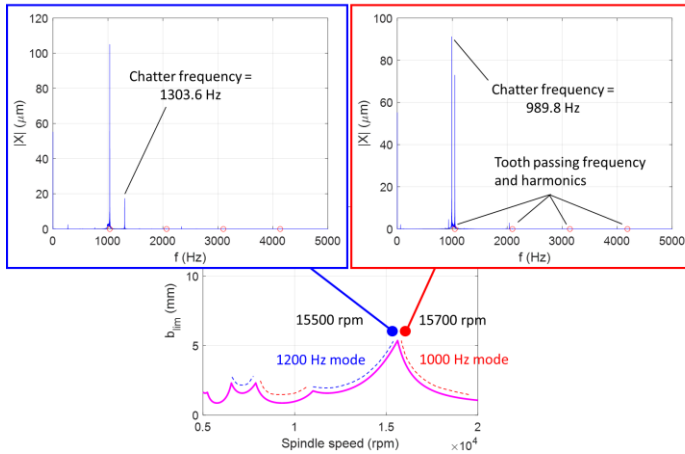


FIGURE 3. Variation in chatter frequency with spindle speed and portion of the stability boundary that is exceeded. The stability map is shown at the bottom, where b_{lim} is the limiting axial depth to avoid chatter, and the insets show the frequency-dependent magnitude of the x direction displacement for the two spindle speeds. The tooth passing frequency and its harmonics are identified by the open red circles.

The initial uniform distributions for the Monte Carlo simulation were defined on the range from 90% of the input variable true value, T , to 130% of T , or $U(0.9T, 1.3T)$. This approach was selected so that: 1) each sample was equally likely to represent the true input value; and 2) the true value was not located at the center of the distribution range.

The six modal parameter distributions were randomly sampled to generate the symmetric tool tip FRFs; see Eq. 5, where f is the excitation frequency (Hz) and F_x is the cutting force in the x direction. The cutting force coefficient distributions were then sampled and combined with the tool tip FRFs to generate 1×10^4 stability maps using the zero-order frequency domain model [2]. The eight input parameters were assumed to be uncorrelated.

$$\frac{X}{F_x} = \frac{1}{k_1} \left(\frac{\left(1 - \left(\frac{f}{f_{n1}}\right)^2\right) - i2\zeta_1 \left(\frac{f}{f_{n1}}\right)}{\left(1 - \left(\frac{f}{f_{n1}}\right)^2\right)^2 + \left(2\zeta_1 \left(\frac{f}{f_{n1}}\right)\right)^2} \right) + \frac{1}{k_2} \left(\frac{\left(1 - \left(\frac{f}{f_{n2}}\right)^2\right) - i2\zeta_2 \left(\frac{f}{f_{n2}}\right)}{\left(1 - \left(\frac{f}{f_{n2}}\right)^2\right)^2 + \left(2\zeta_2 \left(\frac{f}{f_{n2}}\right)\right)^2} \right) \quad (5)$$

Given the 1×10^4 initial stability maps obtained by Monte Carlo simulation, the first test point was selected using the maximum MRR criterion. The result is displayed in Fig. 4, where the spindle speed is 17547 rpm and the axial depth is 3.5082 mm. This maximum expected MRR test point is marked by the white square. The stability map obtained from the true model input values (Table 1) is also included as the magenta curve. This is provided as a reference because it is not known at the time of testing and, therefore, does not influence the test point selection.

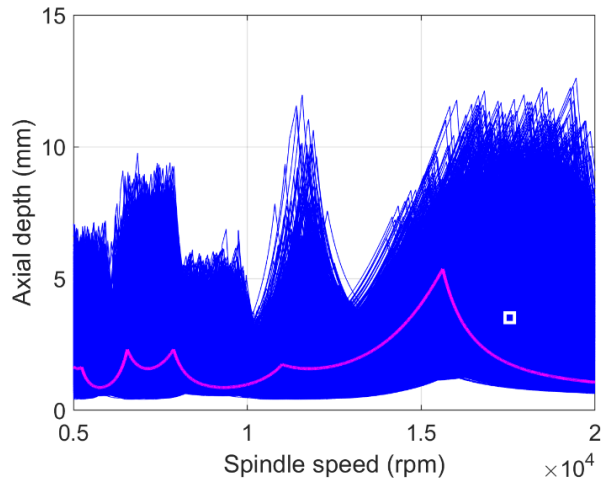


FIGURE 4. Initial distribution of stability maps (blue curves) and first test point (white square). The stability map obtained from the true model input values is included as the magenta curve.

The first test point identified in Fig. 4 is unstable. The corresponding chatter frequency is 1002.4 Hz. The sample partitioning result is displayed in Fig. 5, where it is observed that all stability boundaries below the test point are eliminated and 5933 samples remain after partitioning. Because chatter occurred in the 1000 Hz mode, the f_{n1} distribution accuracy is increased significantly (i.e., those natural frequencies that were far from the true value were effectively eliminated). No appreciable change was observed for the other six distributions (i.e., they remained approximately uniform).

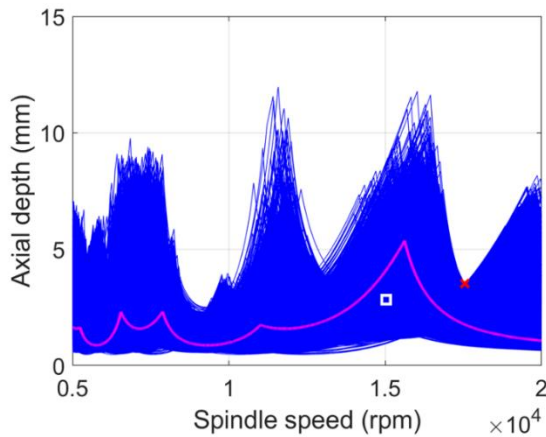


FIGURE 5. Remaining stability maps (5933) after the unstable test at {17547 rpm, 3.5082 mm}; the test point is marked by the red x. The second test point is identified by the white square.

TABLE 2. Testing and sample partitioning results.

Test #	Ω (rpm)	b (mm)	# samples remaining	Result	f_c (Hz)
1	17547	3.5082	5933	U	1002.4
2	15036	2.8313	2284	S	-
3	15652	4.3462	996	S	-
4	15823	5.7928	579	U	990.6
5	14859	4.1948	202	S	-
6	15356	6.3741	117	U	1297
7	19455	1.3065	61	U	1002.3
8	15035	5.2794	39	U	1287
9	19305	1.1535	17	U	1001.4
10	15021	4.8373	9	U	1289.5
11	19343	1.0234	6	S	-
12	15496	5.6584	5	S	-
13	15497	5.7520	2	U	1306.6
14	19599	1.0305	1	S	-

Given the unstable test and corresponding chatter frequency of 1002.4 Hz, the spindle speed for the second test was calculated using Eq. 2. Specifically, $\Omega = \frac{60(1002.4)}{4} = 15036$ rpm. The mean limiting axial depth at the selected spindle speed from the remain stability maps was 2.8313

mm. This test and partion sequence was repeated 14 times until only a single stability map remained. The test points, number of samples remaining after each test, and the chatter frequency, if present, are reported in Table 2.

The sample portioning progression over all 14 tests is summarized in Fig. 6. It is seen how the limited test results quickly refine the initial stability maps distribution. The final map (blue) in panel 14 closely resembles the stability map (magenta) determined using the true values from Table 1. The final values of the stability map input parameters are listed in Table 3. A comparison to the true values is provided.

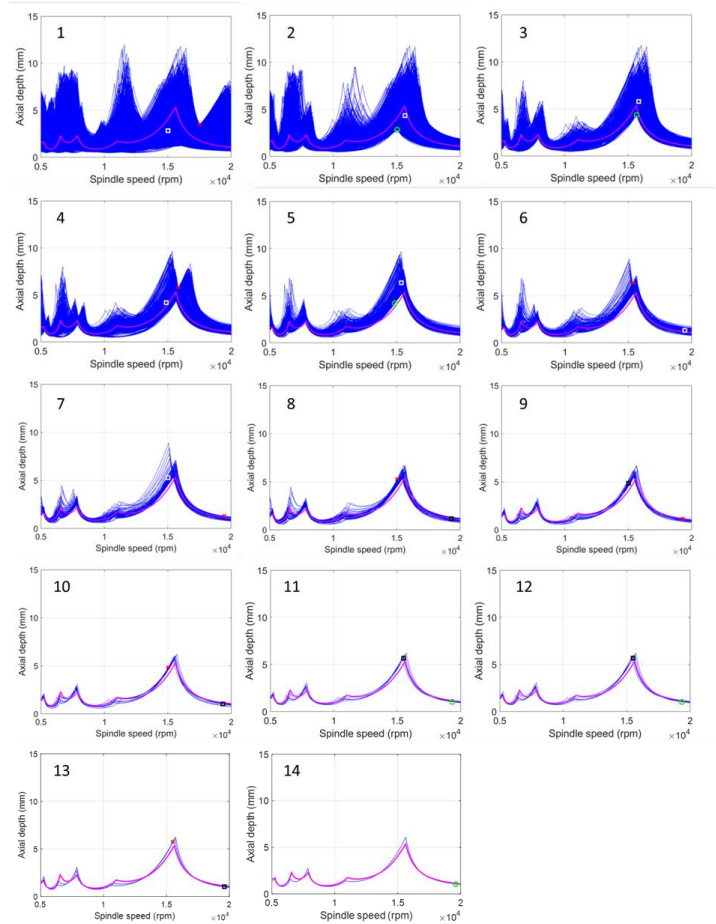


FIGURE 6. Sample partitioning results for each test. The remaining maps after each test are shown where the green circle or red x indicates if the test was stable or unstable. The next test point is identified by the square (white or black to provide the best visibility).

DISCUSSION

As seen in Fig. 6, the sample partitioning approach effectively reduces the initial 1×10^4

stability maps to a single sample using only 14 tests. Furthermore, the remaining map accurately represents the map obtained from the true model input values. In practice, however, all 14 tests may not be required. The user could elect to discontinue testing at any point using an appropriate stopping criterion. The criterion could be based on the remaining number of samples, changes to the distribution, or test cost, for example. In an *ad hoc* sense, a review of Fig. 6 suggests that tests 8 or 9 could serve as a stopping point since the basic shape of the stability boundary has been identified.

TABLE 3. Comparison of stability model inputs after sample partitioning (14 tests) and the true values.

Stability model input	Post-partitioning	True	Percent difference
f_{n1} (Hz)	1015.1	1000	1.51
k_1 (N/m)	5.5233×10^6	5×10^6	10.47
ζ_1 (-)	0.021	0.02	5.00
f_{n2} (Hz)	1143.1	1200	-4.74
k_2 (N/m)	8.3542×10^6	7×10^6	19.3
ζ_2 (-)	0.028	0.03	-6.67
k_t (N/mm ²)	872.75	700	24.7
k_n (N/mm ²)	232.71	200	16.4

presence of the two modes did not limit the algorithm efficiency.

An interesting result was obtained for test 12 as shown in Fig. 7. While the selected test point exceeded the stability boundary defined by the true stability model input parameters, the test point was stable as determined by time domain simulation. This highlights that approximations are applied to obtain the time invariant, radial immersion-dependent milling model [2]. Although the model is generally accurate, discrepancies with tests may occur. The sample partitioning therefore serves to select those stability maps that best agree with the test results, not necessarily those that are generated from input parameters that best match the true values. This is emphasized by the Table 3 results, where disagreement between the final and true stability model inputs is observed, but the final stability map provides good agreement with both the test results and the stability map obtained from the true input values.

After testing is concluded, the remaining stability maps represent the model for parameter selection. If multiple maps are retained (e.g., 39 samples would remain if testing was discontinued after test 8), then multiple values for each model parameter would remain. The mean values of the modal parameters and cutting force model coefficients at each spindle speed could be calculated, for example, and then used to define the stability map. The final milling parameters would then be based on the user's risk preference. Most likely, combinations of {spindle speed, axial depth} at the stability boundary would not be selected since it is understood that uncertainty remains, even though it has been reduced by the testing and sample partitioning. It is important to note that the stability map input values identified by testing and sample partitioning can be applied to other milling conditions. For example, the milling direction could be switched from down to up milling and the radial depth could be changed. In this way, the method is generalizable to other milling conditions.

To evaluate the parameters from Table 3, time domain simulation results are compared for up milling with a 5 mm radial depth of cut and 0.15 mm feed per tooth. Recall that the model was developed using a 3 mm radial depth of cut for down milling with a 0.1 mm feed per tooth. To choose the {spindle speed, axial depth}

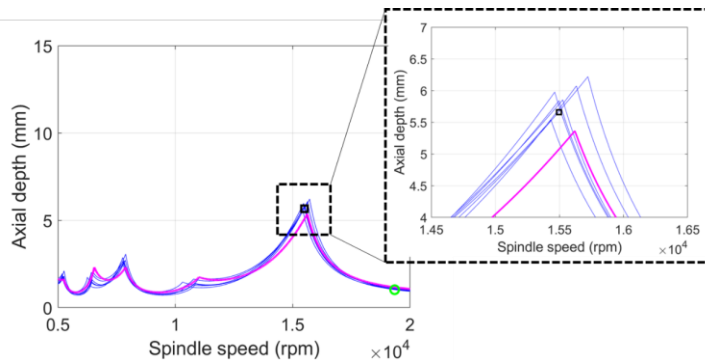


FIGURE 7. Point 12 from Table 2 is identified by the black square. Although the result is predicted to be unstable using the stability map predicted from the true model inputs (magenta), it was observed to be stable in the time domain simulation, which provided the test result for this study.

A second observation is that the chatter frequency-based spindle speed selection enabled the domain to be explored and the uncertainty to be reduced. For the case study, the two mode system caused the chatter frequency to vary between spindle speeds near 15000 rpm and 19000 rpm; see Table 2 and Fig. 6. The

combinations for testing, the stability map was calculated using the frequency domain model [2] and post-partitioning input values from Table 3. Tests were then performed at the spindle speed corresponding to the maximum allowable axial depth from the predicted stability map.

A comparison of the results using the true and post-partitioning values is shown in Fig. 8, where the test spindle speed was 15663 rpm. The axial depths were 3 mm and 4 mm. The stability map for the true values (magenta) predicts the 3 mm axial depth to be stable and the 4 mm axial depth to be unstable. The post-partitioning stability map (blue) predicts both axial depths to be stable; the local peak in this map is located at {15663 rpm, 4.41 mm}. The left inset shows that the 3 mm axial depth is stable for both parameters set. Due to the larger cutting force coefficients for the post-partitioning results, the corresponding x direction force, F_x , is larger (blue). Because the force is larger, the x direction vibration response (blue) is also larger. The circles represent the once-per-tooth samples. Because they repeat from one tooth passage to the next, forced vibration is present and the cutting conditions are stable [4].

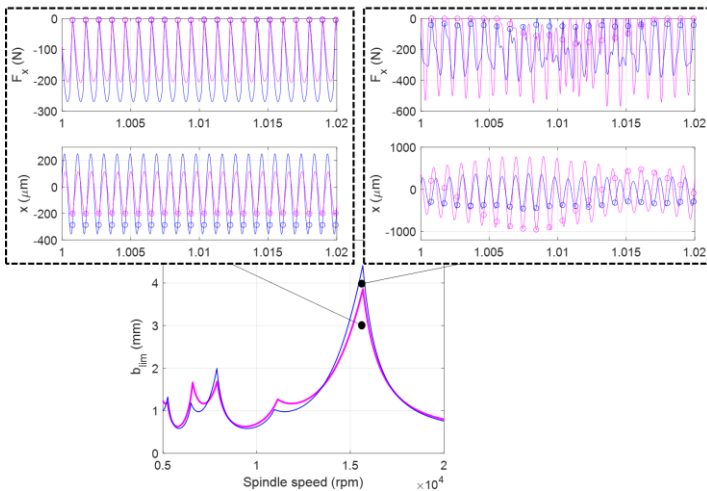


FIGURE 8. Comparison of results using the true (magenta) and post-partitioning (blue) values.

CONCLUSIONS

This paper described a milling modeling approach that implemented sample partitioning to retain or reject samples from an initial distribution of stability maps using milling test results. Because the stability model input parameters are also partitioned using the test results, their uncertainty is reduced using the test results and the milling stability model accuracy is increased. In a case study, the stability maps were

calculated from distributions of uncertain: 1) modal parameters that represent the tool tip frequency response functions; and 2) cutting force model coefficients. Test points were selected based on the previous test result. If the previous test was stable, the combination of spindle speed and mean axial depth from the remaining samples that provides the high material removal rate was selected. If the previous test was unstable, the spindle speed for the next test was calculated using the chatter frequency, where the tooth passing frequency was set equal to the chatter frequency. The mean axial depth at that spindle speed was then selected to fully define the test point.

A case study validated the approach. For a selected milling system, defined by a two-mode symmetric frequency response function and mechanistic cutting force model, initial uniform distributions for the stability model input parameters were reduced from 1×10^4 samples to a single final sample in only 14 tests. The remaining stability map provided good agreement to the stability map produced from the true model input values. A discussion was provided that explored stopping criteria, multiple chatter frequencies, disagreement between time domain simulation (used for testing here) and the frequency domain stability model, and final milling parameter selection given the reduced uncertainty model after testing, including generalizability.

ACKNOWLEDGEMENTS

The author gratefully acknowledges support from MxD (Manufacturing x Digital) and the NSF Engineering Research Center for Hybrid Autonomous Manufacturing Moving from Evolution to Revolution (ERC-HAMMER) under Award Number EEC-2133630.

REFERENCES

- [1] Altintas, Y., Stepan, G., Budak, E., Schmitz, T. and Kilic, Z.M., 2020. Chatter stability of machining operations. *ASME Journal of Manufacturing Science and Engineering*, 142(11), p.110801.
- [2] Altintas, Y. and Budak, E., 1995. Analytical prediction of stability lobes in milling. *CIRP Annals*, 44(1), pp. 357-362.
- [3] Schmitz, T. and Smith, K.S., 2019. *Machining Dynamics: Frequency Response to Improved Productivity*, Second Edition. Springer.
- [4] Honeycutt, A. and Schmitz, T.L., 2017. Milling stability interrogation by subharmonic sampling. *Journal of Manufacturing Science and Engineering*, 139(4), p.041009.